A DIGITAL ELEVATION MODEL OF MIRANDA'S YOUNGEST CORONA, INVERNESS.

C. B. Beddingfield[1,2]; E. J. Leonard[3], C. M. Elder[3], T. A. Nordheim[3], R. J. Cartwright[1], C. Cochrane[3], L. Regoli[4], and D. Atkinson[3]. (chloe.b.beddingfield@nasa.gov) [1]SETI Institute, [2]NASA Ames Research Center, [3]Jet Propulsion Laboratory, California Institute of Technology, [4]John Hopkins University Applied Physics Laboratory, MD

Background: Miranda is the innermost and smallest of the classical Uranian satellites, with a ~470-km-mean-diameter [1]. This satellite has a geologically complex and highly deformed surface, highlighted by regions of tectonically resurfaced terrain with low crater densities, termed "coronae" and a large system of normal fault scarps up to 8 km in height making up the "Global Rift System," present within the cratered terrain (**Figure 1**) [2,3]. Verona Rupes, the 340 Degree Chasma, and the South Pole Tangent Chasma are part of the Global Rift System [3], along with numerous smaller scale faults and fractures across the cratered terrain.

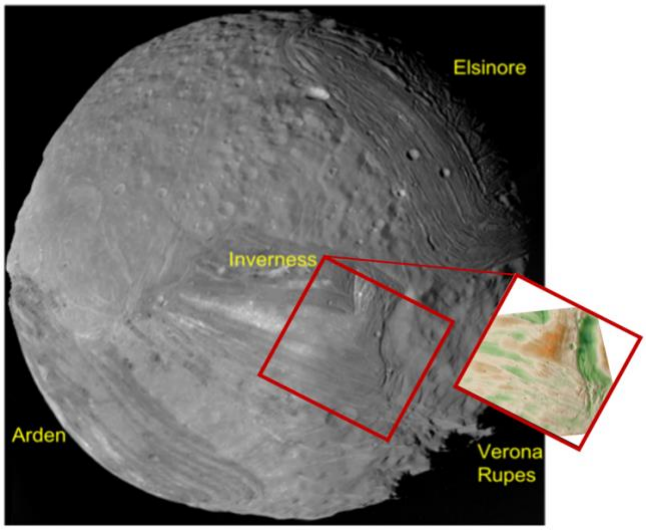

Figure 1. *Modified figure from [4], showing the location of Miranda's coronae and the digital elevation model (**Figure 2**).*

Miranda's coronae are polygonal shaped in plan view and are separated from the surrounding cratered terrain by sets of large sub-parallel linear features. As summarized in [3], multiple processes have been suggested for the formation of the coronae, including: relaxation of topographic highs, lithospheric stress driven by density anomalies in the asthenosphere, diapirs breeching the surface, large-scale volcanic flooding through pre-existing cracks, and interior convection [5-8]. The formation of Miranda's coronae may have occurred due to tidally generated heating, as Miranda passed through orbital resonances with neighboring Umbriel and/or Ariel [3, 9-11]. Evidence for these resonances include Miranda's inclined orbit (i ~4.34°), which is notably higher than that of the other classical moons (i < 0.13°) [12].

In our ongoing work, we are investigating Inverness Corona, the youngest corona on Miranda [13], to improve our understanding of the most recent geologic activity on this moon, and how this activity might be linked to endogenic processes, such as tectonism and cryovolcanism [e.g. 4]. Although Voyager 2 only imaged approximately half of Miranda's surface, the full spatial extent of Inverness Corona was captured during the flyby, unlike Arden and Elsinore Coronae, which were only partially imaged. Consequently, morphometric analysis of Inverness Corona could reveal key insight into Miranda's most recent geologic history. Here, we present a new digital elevation model (DEM) of Inverness Corona, which we will use to further analyze Miranda's geologic history.

Digital Elevation Model: We generated a DEM using Voyager 2 Imaging Science Subsystem (ISS) images c2684617 and c2684629, which cover a large section of Inverness Corona (**Figure 2**). The ISS images incorporated into the DEM were processed using the Integrated Software for Imagers and Spectrometers (ISIS) [14]. We then used a combination of stereogrammetry (see [15] for methodology details) and photoclinometry (PC) techniques to derive topographic information. For PC, the brightness value of a pixel is a function of solar and viewing geometry and used to interpret the value of a topographic slope. A photometric model of Miranda's surface was taken as a sphere with a radius equal to that of Miranda using the lambertian photometric model. The topographic slopes calculated for each pixel were incorporated into the digital elevation model.

To access the accuracy of the resulting topography, we investigated shadow measurement techniques, discussed in [e.g., 16], to independently estimate the heights of ridges and depths of impact craters. The shadow measurements were conducted to determine topographic information in select regions. Additionally, we investigated the depth-diameter ratio of a large impact crater covered by the DEM, to determine if this ratio is consistent with those measured previously for other impact craters on Miranda [17] (**Figure 3**). Our results show that the impact crater covered by the DEM has a depth of ~1.4 km and a diameter of ~6.9 km (depth-diameter ratio of

0.2), which is a similar ratio with those estimated in previous work for craters on Miranda [17].

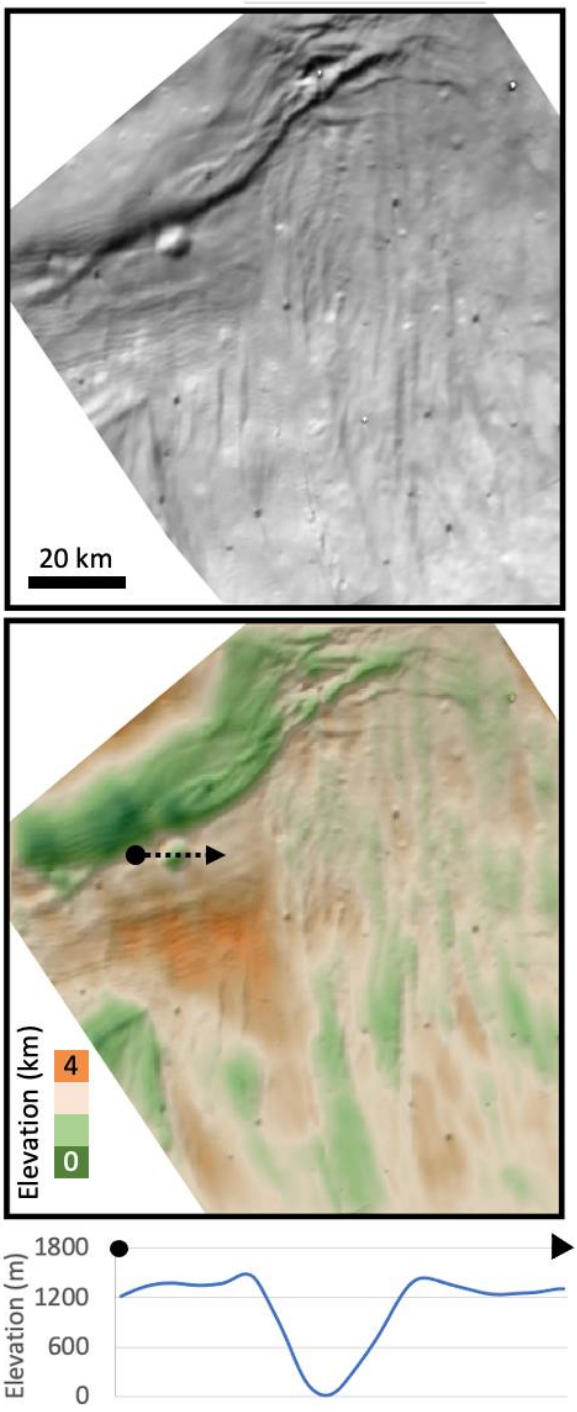

Figure 2. *Inverness Corona reflectance image (top), digital elevation model (middle), and an impact crater profile (bottom). The diameter of the crater is 6.9 km.*

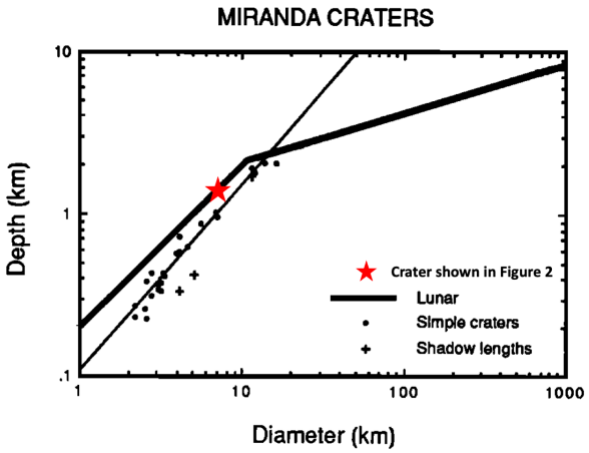

Figure 3. *Modified figure from [17] that includes the depth and diameter of the impact crater shown in Figure 2 (red star). The depth diameter ratio of this crater is 0.2, consistent with those observed elsewhere on Miranda.*

Future Work: We will use this DEM to investigate recent geologic activity on Miranda, including the tectonic processes that formed Inverness Corona. We will us use the geometries of Inverness' large set of normal faults to constrain the heat flux of Miranda that was present during the formation of this terrain. We will then compare our results to the heat fluxes expected if a subsurface ocean was present in this region during the formation of Inverness Corona.

Acknowledgments: This research was funded by a subcontract grant to Chloe Beddingfield with the Jet Propulsion Laboratory (SI-2021-028-yr1) and the National Aeronautics and Space Administration.

References: [1] Thomas P. C. (1988) *Icarus*, *73*, 427-441. [2] Croft S. K. and Soderblom L. A. (1991) *Uranus*, 561-628. [3] Greenberg R. J. (1991) *Uranus*, 693-735. [4] Beddingfield C. B. and Cartwright R. J. (2020) *Icarus*, 343, 113687. [5] Johnson T. V. et al. (1987) *Scientific American*, 256, 48-61. [6] Schenk P. M. (1991) *JGR: Solid Earth*, 96, 1887-1906. [7] Pappalardo R. T. et al. (1997) *JGR: Planets*, 102, 13369-13379. [8] Hammond N. P. and Barr A. C. (2014) *Geology*, 42, 931-934. [9] Dermott S. F. et al. (1988) *Icarus*, 76, 295-334. [10] Tittemore W. C. and Wisdom J. (1990) *Icarus*, 85, 394-443. [11] Ćuk M. et al (2020) *PSJ*, 1:22, 19. [12] Laskar J. and Jacobson R. A. (1987) *Astron. and Astrophys.*, 188, 212-224. [13] Zahnle K. et al. (2003) *Icarus*, 163, 263-289. [14] Anderson J. A. et al. (2004) *LPSC*, 35, 2039. [15] Beddingfield C. B. et al. (2015) *Icarus*, 247, 35-52. [16] Dameron A. C. and Burr D. M. (2018) *Icarus*, 305, 225-249. [17] Schenk P. M. (1989) *JGR: Solid Earth*, 94, 3813-3832.